Dynamics of a Highly Charged Ion in Aqueous Solutions: MD Simulations of Dilute $CrCl_3$ Aqueous Solutions Using Interaction Potentials Based on the Hydrated Ion Concept

José M. Martínez,[†] Rafael R. Pappalardo,[†] Enrique Sánchez Marcos,*[,†] Keith Refson,[‡] Sofía Díaz-Moreno,[#] and Adela Muñoz-Páez[#]

Departamento de Química Física, Facultad de Química, Universidad de Sevilla, 41012-Sevilla, Spain, Department of Earth Sciences, Oxford University, Oxford OX1 3PR, UK, and Departamento de Química Inorgánica, Facultad de Química, Universidad de Sevilla e Instituto Ciencia de Materiales, Centro Cartuja, CSIC, Spain

Received: November 13, 1997; In Final Form: February 4, 1998

Structural and dynamical properties of dilute aqueous solutions containing a trivalent cation have been determined by means of Molecular Dynamics simulations. The concept of hydrated ion has been used when considering aqueous solutions of Cr^{3+}, $[Cr(H_2O)_6]^{3+}$ being the cationic entity interacting in solution. An ab initio Cr^{3+} hydrate−water interaction potential previously developed [*J. Phys. Chem.* **1996**, *100*, 11748] and a new one describing the Cr^{3+} hydrate−Cl^- interactions have been used with a TIP4P water model to carry out simulations of the system $Cr(H_2O)_6Cl_3 + 512H_2O$. To examine the role of anions, simulations without chloride ions were performed as well ($[Cr(H_2O)_6]^{3+} + 512H_2O$). To investigate the influence of shape and size of the hydrated cation, two additional models of trivalent cation have been studied using the simplest concept of spherical ion. Ad hoc charged sphere−water interaction potentials for the latter situations were built. RDFs, hydration numbers, vibrational spectra of the intermolecular modes, translational self-diffusion coefficients for ions and water molecules in the different hydration shells, interdiffusion coefficients, mean residence times, and rotational diffusion coefficients and correlation times for the hexahydrate and water molecules are obtained and discussed. Comparison of dynamical properties of Cr^{3+} aqueous solutions with those obtained from simulations of Cr^{3+} hexahydrate strongly supports the validity of the hydrated ion model for this cation. The examination of rotational mobility leads to the conclusion that the hydrate ion rotates following Debye's rotational model. Advantages and drawbacks of the hydrated ion approach to deal with solvation of highly charged cations of transition metals are examined. The structural consequences of adopting a spherical shape for cation when developing potentials are quite different when either the bare or hydrated radius is considered; thus, whereas the small sphere overestimates the first shell coordination number, the big sphere overestimates the second hydration shell, promoting a clathrate structure. Specially designed EXAFS measurements of a set of $Cr(NO_3)_3$ aqueous solutions 0.1 M in hydrochloric and hydrobromic acids were carried out and analyzed to investigate the possibility of detecting the halide anion in the first or second hydration shell. Simulations agree with experimental results in the sense that the counterion of Cr^{3+} hexahydrate is placed in dilute acidic solutions beyond the second hydration shell.

Introduction

Computer simulations based on the use of statistical methods such as Monte Carlo and Molecular Dynamics have improved our understanding of the liquid state during the last two decades.[1−4] The ionic solution field has especially profitted from these developments.[5−7] In earlier theories of electrolytes, the presence of charged particles has been a challenge for researchers as thermodynamics properties of ionic solutions must be obtained on the basis of individual ionic contributions which necessarily use some extra-thermodynamical assumptions founded on a microscopic model. Primitive models used spherical shape for ions and electrostatic theory of condensed media to give a reasonable representation of the system.[8−10] Following this scheme, the intermolecular interaction potentials employed in the statistical simulation of solutions containing monatomic ions are mainly adapted to the shape and electric properties of the solvent considered. The most desirable, although costly, strategy to establish intermolecular interaction potentials is their extraction from quantum chemical potential energy surfaces; in such a way one can test the reliability of modeling ionic solutions upon first-principles-based statistical simulations.[3] Calculations of structural and dynamical properties of ionic aqueous solutions showed that pairwise additive intermolecular potentials, which are not empirically corrected, are generally unable to represent adequately ion−polar solvent interactions.[11] It is due to the important role played by interaction energies such as polarization and charge transfer whose contributions to the whole potential are not pairwise additive. Several techniques have been proposed and applied in the literature to include these interactions. Elrod and Saykally have recently reviewed the many-body effects in the intermolecular forces and we refer to this work for a global vision of the topic.[11] Within the particular domain of multivalent cation hydration, some interesting works have just appeared dealing with this topic from different

[†] Universidad de Sevilla.
* Corresponding author. E-mail: sanchez@mozart.us.es.
[‡] Oxford University.
[#] Universidad de Sevilla e Instituto Ciencia de Materiales.

S1089-5647(98)00196-5 CCC: $15.00
Published on Web 04/02/1998

approaches. Thus, the Zn^{2+} hydration has recently been revisited adding a water−ion−water three-body contribution term to an ab initio ion−water potential.[12] Inclusion of polarizable water models has also been used to account for the hydration of divalent and trivalent cation from MC and MD simulations.[13−15] Yet another approach is to extract effective pair potentials from calculations of the interaction of a water molecule with a cation already solvated by other water molecules, either defining a continuum model[16] or averaging the interaction of the cation with a water cluster which describes the first hydration shell.[17,18]

The most complex situation usually appears in highly charged metallic cations that generally impose a well-defined solvent structure around them. Even more, in some cases, mainly among transition-metal cations, the solvated ion formed should be envisaged as a coordination complex.[19,20] Bearing in mind these physicochemical features and the concentric solvation shell model proposed by Frank and Evans,[21] we have recently proposed the use of the hydrated ion as the entity to be considered in the determination of the ion−water interaction potential, and then in simulations of aqueous solutions containing transition-metal cations. First of all, an ab initio interaction potential between the Zn^{2+} hexahydrate and a water molecule, $[Zn(H_2O)_6]^{2+}-H_2O$, was built.[22] MC simulations gave a reasonable structural and energetic description which compelled us to study the more involved problem of the Cr^{3+} hydration. In this case, the hydrated ion approach is particularly adequate because of the high stability of the $[Cr(H_2O)_6]^{3+}$ complex in water.[6a] A Monte Carlo simulation of Cr^{3+} in water has already been published.[23] The results have confirmed the suitability of the suggested approach. In that work, we also examined shortcomings of the hydrated ion−water potential such as the remaining many-body effects within this model. Likewise, the influence of the nonflexible character of our hydrate on the static and energetic properties has recently been tackled by us.[24] The highly charged small spherical cation, sometimes replaced by a medium or large sphere accounting for the hydration,[25] is in the actual solution model replaced by a polyatomic ion with a complex shape and charge redistribution.[22,23]

Bleuzen et al.[26] have recently published a study on the water-exchange mechanism of Cr^{3+} aqueous solutions. They have performed MD simulations using an ion−water potential based on the use of the hydrated ion concept, where the water molecules of the first shell are described by a modified TIP3P model fitted to reproduce some experimental results. Comparison between both types of simulations will be done to get insight into the fundamental aspects of the potential approach employed as well as the simulation conditions and the analysis of the results. Likewise, Wasserman et al.[27] have very recently used the same concept to obtain from MD simulations energetic and structural data for the Al^{3+} hydration.

The aim of this work is to investigate the ability of the hydrated ion approach to describe the dynamic properties of ionic aqueous solutions. It is of interest to point out that the potential employed is based on first-principles so that the verification of its suitability by describing concurrently static, dynamic, and energetic properties must be a valuable check on this type of strategy to simulate solutions containing highly charged metallic cations. To get an insight into the physical foundations of the hydrated ion model, the role of the counterion has been examined by performing simulations with and without chloride anions. A set of EXAFS measurements has also been carried out in order to supply experimental information on the position of counterions in Cr^{3+}-containing aqueous solutions. Previously, the possibility of determining the structure of the second hydration shell from EXAFS spectra has been shown,[28] as well as the presence of chloride ions in this second shell, in addition to the first shell, for hydrochloric acid aqueous solutions of $[CrCl_x(H_2O)_{6-x}]^{(3-x)+}$ complexes.[29] EXAFS spectra of $Cr(NO_3)_3$ aqueous solutions which have been acidified by small amounts of hydrochloric or hydrobromic acid have been recorded. The starting hypothesis is that, if chloride or bromide anions occupy the first or the second shell, they should be detected, as chloride anions were already detected in the previous experiments.[29]

A final aim of the work is to examine the results obtained from two models of solution where the trivalent cation has been represented by a soft sphere, in one case with a radius representing the bare ion, and in the other case, the hydrated ion. Comparing these results to those obtained by a more detailed structural description, as the hydrated ion, the importance of the charge distribution is thoroughly examined and some comments about phenomenological models based on Born formulation and the microscopic interpretation of ionic radius may be substantiated.[5,25]

Methodology

EXAFS Measurements and Data Analysis. EXAFS measurements of the Cr−K edge at 5989 eV were carried out at the Photon Factory synchrotron radiation source (KEK) in Tsukuba (Japan) at beamline 12C. Ring current was 300 mA and ring energy 2.5 GeV. A high-resolution Si(111) double crystal monochromator was used, followed by a Rh-coated Si focusing mirror. Higher harmonic rejection was carried out with a SiO2 total reflection mirror, and energy calibration with a Cr foil. Data were collected in the transmission mode using ionization chambers as detectors. At least four scans were recorded to minimize high- and low-frequency noise. Liquid samples were placed in special liquid cells that allow the recording of highly corrosive media with variable path length.[30]

The EXAFS functions $\chi(k)$ were obtained from the X-ray absorption spectra by subtracting a Victorieen curve (pre-edge absorption) followed by a cubic spline background removal (atomic absorption) using the program XDAP.[31] Normalization was done dividing by the height of the edge, and E_0 was defined as the maximum of the first derivative of the absorption edge. Three sets of phase shift and backscattering amplitude functions for Cr−O contribution were used. Two were obtained from the experimental spectrum of the solid crystalline hydrate, $[Cr(NO_3)_3]\cdot 9H_2O$, and a third one was calculated using FEFF 6.01 code (see the following section).[32] To calculate the last one, the amplitude reduction factor S_0^2 and the Debye−Waller factor were set equal to 0.9 and 0.0, respectively. Errors in the structural parameters were calculated from the covariance matrix taking into account the noise in the experimental EXAFS spectra and the correlation between the refined parameters. The quality of the fit was quantitatively determined by the goodness-of-fit value, (ϵ_ν^2).[33]

Intermolecular Potentials. $[Cr(H_2O)_6]^{3+}-H_2O$ intermolecular potential building has already been explained in a previous paper.[23] However, for the MD simulations the water model has been changed. The TIP4P model[34] has substituted the MCY one[35] since it is generally accepted that the former gives a better description of bulk water properties, and the molecular geometry is the same for both models, i.e., the experimental one. This last fact allows us the modification of the original $[Cr(H_2O)_6]^{3+}-H_2O$ potential with minimal changes. In this sense, the Coulombic part is the only term that has been

TABLE 1: Summary of the Performed Simulations

simulation code	system	potentials	collection periods
A	$[Cr(H_2O)_6]^{3+} + 3Cl^- + 512H_2O$	HIW, HICl, OPLS, TIP4P	4 runs of 200 ps
B	$[Cr(H_2O)_6]^{3+} + 512H_2O$	HIW, TIP4P	4 runs of 200 ps
C	[small soft sphere]$^{3+}$ + $512H_2O$	Q3S, TIP4P	2 runs of 150 ps
D	[big soft sphere]$^{3+}$ + $512H_2O$	Q3B, TIP4P	2 runs of 150 ps
E	$512\ H_2O$	TIP4P	1 run of 200 ps

modified: the MCY charges of the water molecule were replaced by those corresponding to the TIP4P potential. The general expression for the hydrated ion−water potential (HIW) becomes:

$$E_{\mathrm{HIW}} = \sum_{i}^{\text{HI sites}} \sum_{j}^{\text{W sites}} \frac{C_4^{ij}}{r_{ij}^4} + \frac{C_6^{ij}}{r_{ij}^6} + \frac{C_{12}^{ij}}{r_{ij}^{12}} + \frac{q_i q_j}{r_{ij}} \qquad (1)$$

The coefficients for this HIW potential are given in the Supporting Information. The goodness of the fit is similar to that found for the original potential.[23]

In order to take counterions into account in our simulation, an interaction potential between the HI and the Cl^- ion has been developed. For that, an ab initio potential energy surface of this system has been explored in a similar way to that described in previous papers.[22,23] For the chlorine atom, the 6-31+G* basis sets was employed. Due to the atomic character of the anion, the total number of points used for the fitting was 400 (cf. with the 1200 points needed to fit the HIW potential). The functional form was the same as that of the HIW (eq 1): r^{-4}, r^{-6}, r^{-12}, and Coulombic terms, where the *j* index only runs on the Cl site. (Coefficients for this HICl potential are given in the Supporting Information.) The standard OPLS potential for the interaction chloride−water was employed.[36]

For comparative purposes two additional cation−water interaction potentials have been considered. In both cases, the cation has been modeled by soft spheres (Lennard-Jones potential) with different effective radii and a Coulombic term:

$$E_{\mathrm{SW}} = 4\epsilon\left[\left(\frac{\sigma}{r_{q\mathrm{O}}}\right)^{12} - \left(\frac{\sigma}{r_{q\mathrm{O}}}\right)^{6}\right] + \sum_{j}^{\text{W sites}} \frac{q_q q_j}{r_{qj}} \qquad (2)$$

where $q_q = +3$ and q_j refers to the TIP4P point charges. The σ values were chosen such that the minimum for the pair potential appears in one case at the chromium−oxygen distance of the first hydration shell ($Cr-O_I = 2.05$ Å),[23] and in the other case at the first maximum of the Cr−O RDF for the Cr^{3+} hexahydrate MD simulation ($Cr-O_{II} = 4.06$ Å). The ϵ values were obtained from the interaction ab initio energy[37] of a triple charge point and a water molecule with the experimental geometry, subtracting the electrostatic part. The values for these potentials are given in the Supporting Information. These two simple potentials are rough approximations to the bare and the hydrated ion. Hereafter, the first potential will be termed Q3S (i.e., charge 3+ small sphere) and the second one, Q3B (i.e., charge 3+ big sphere).

Simulation Details. Molecular dynamics simulations were performed in the microcanonical ensemble using periodic boundary conditions; 512 TIP4P water molecules were used as solvent and, depending on the case, solute entities were either the hydrated cation $[Cr(H_2O)_6]^{3+}$ and $3Cl^-$, or only $[Cr(H_2O)_6]^{3+}$, or the triple charge soft sphere with the small radius or the big one. In addition, a simulation containing just 512 water molecules has been carried out for comparative purposes to determine the water properties in the pure solvent obtained under our simulation conditions. The basic cell was in all cases a cubic box with sides of 24.8 Å, which gives a density of 1 g/cm^3 for the pure water simulation, and values ranging from 1.02 to 1.03 g/cm^3 for the ionic solutions. Table 1 terms and summarizes the set of performed simulations.

Simulations were run with the Moldy program[38] (Version 2.10) slightly modified to incorporate the short-range part of the functional form of eq 1; later versions of the code already include such a potential. Newton−Euler equations of motion were integrated using a modified form of the Beeman algorithm[39,40] which is known to guarantee a good stability for molecular systems. Orientations of rigid molecules were handled by means of the quaternion formalism[41] and the time step chosen was 0.25 or 0.30 fs, depending on the system.

Coulombic interactions were computed using the Ewald sum technique,[1] including the charged system term where necessary.[38,43] The importance of this treatment has been shown to provide reliable structural and, particularly, dynamical results in the case of ionic aqueous solutions.[42−44] A spherical molecular cutoff was applied to the real space part of the Ewald energy as well as the short range potential. The Moldy program implements the link cell method[2,45] to treat this kind of interaction which allows cutoff larger than *L*/2. This was necessary in the case of samples containing the HI where a cutoff of 15 Å was applied. For the remaining cases, a cutoff of *L*/2 was used. Corrections to the potential energy and pressure arising from the use of the cutoff were included.

Configurations from the previous Monte Carlo runs[23] were used as the initial states for the simulations of pure water and $[Cr(H_2O)_6]^{3+} + 512H_2O$. Subsequent runs were started from an equilibrated state at 298 K of the latter system, changing, if necessary, the nature of the cation (HI to Q3S or Q3B). For the case of the situations where Cl^- anions were used, they were added randomly to the equilibrated box. Thermalization time was about 40 ps for the first run of each kind of simulated sample.

As indicated, all simulations, except E, were divided in statistically different runs. In order to achieve such a condition, a small reequilibration period was applied between subsequent runs of the same system. Trajectories and velocities were saved every 40 time steps. Computations were carried out with the aid of a parallel CONVEX-Exemplar SPP-1000 Series and a HP-9000/735 (99 MHz). On this latter computer a step consumed about 13 s.

Results and Discussion

Structural Properties. *MD Simulation Data.* Figure 1a shows the radial distribution function (RDF) for the Cr−O and Cr−H pairs of simulation A that contains the hydrated ion and its counterions. Obviously, since the first hydration shell is implicit in the cation for simulation A, as well as for B and D, the values of the function for Cr−O and Cr−H are 0 up to ca 3.7 Å. Running integration numbers have also been included in the figure. The Cr−O RDF shows a sharp peak at 4.07 Å for simulation A which indicates the presence of a well-defined second hydration shell for Cr^{3+} aqueous solutions. The integra-

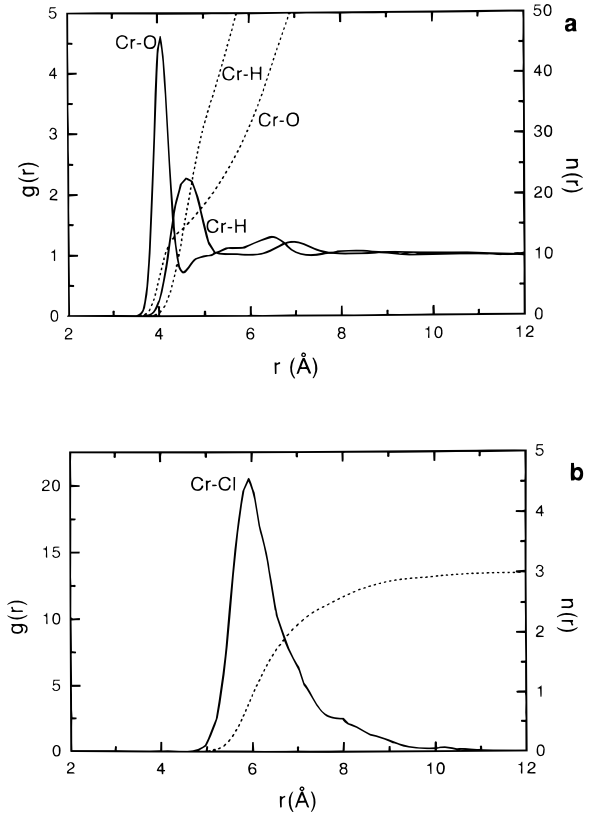

Figure 1. Results of simulation A: (a) Cr−O and Cr−H RDF (solid line) and their running integration numbers (dashed line). (b) Cr−Cl RDF (solid line) and its running integration number (dashed line).

tion number of this peak leads to 14 water molecules. The Cr−H RDF presents the corresponding second hydration shell peak with a maximum at 4.65 Å and an integration number of ca. 32. These results compares well with the spectroscopic results of Cr^{3+} salt aqueous solutions obtained by LAXS,[46] XRD,[47] ND,[48] and EXAFS,[28] as well as with the results derived from the fitting of the EXAFS spectra presented below.

It is worth mentioning that the RDFs for the same pairs in simulation B, where anions are excluded, almost match. That is, the strong structural character of the trivalent cation in water highly dominates its close surroundings. The RDF for Cr−Cl corresponding to simulation A (Figure 1b) helps us to understand this structural result. Chloride anions occupy a region beyond the second hydration shell. In fact, the maximum of its RDF is found at ca. 5.94 Å. At first sight this result seems to be surprising given the intense electrostatic forces between Cr^{3+} and Cl^- and the small size of anion, which would allow an easy insertion in the nearest hydration shells to the cation. To check this finding, the analysis of a set of EXAFS spectra of Cr^{3+} aqueous solutions containing halides is presented below. It shows that halides are not detected in the two first hydration shells. Likewise, Bleuzen et al.[26] have found in their recent MD simulations of $Cr(ClO_4)_3$ aqueous solutions that perchlorate anions never enter the second hydration shell. Nevertheless, the size of this polyatomic anion makes its insertion in these shells more difficult than for halides.

The orientational features of water structure when it moves further off the hydrated cation are represented in Figure 2 by means of the change of the angle θ formed by the ion−oxygen vector and the water dipole vector. Thus, a value close to 180° indicates a strong alignment around cation, whereas 90° is the asymptotic value for a cation-independent structure. Angle functions for simulations A and B almost overimpose up to 5.2

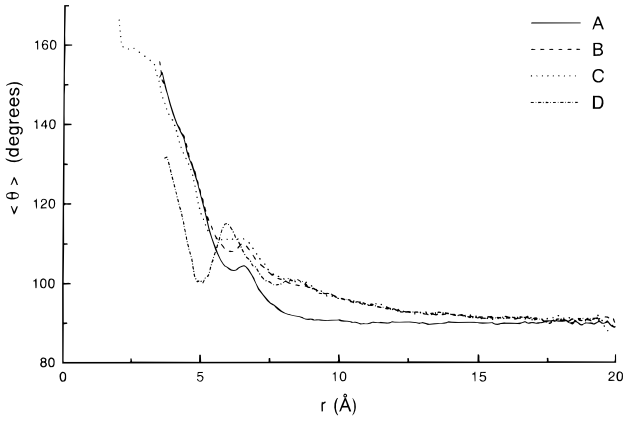

Figure 2. Mean value of the angle θ, formed by the ion−oxygen vector and the water dipole vector, as a function of the ion−oxygen distance.

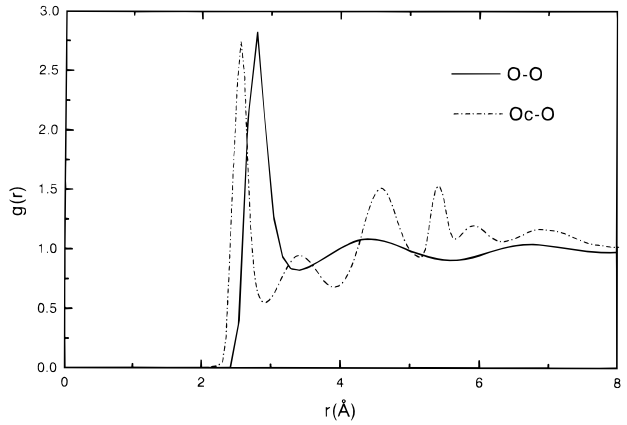

Figure 3. Oxygen−oxygen RDF of the pure water simulation (solid line) and oxygen of the hydrate (O_c)−oxygen of the free water molecules (O) RDF of simulation A (dashed line).

Å. This angle value indicates a strong solvent structure-breaking character of the hydrated cation up to the second hydration shell. Beyond that, the presence of chlorides in simulation A leads to a more pronounced loss of ordering around the cation. A similar behavior is found for La^{3+} when a set of MD simulations with and without Cl^- anions are compared.[49] The hump observed around 6−7 Å corresponds to the presence of an ill-defined third hydration shell that also appears in the Cr−O and Cr−H RDFs (Figure 1).

Figure 3 shows the O_c−O RDF which gives the distribution of oxygen atoms of free water molecules (O) around the oxygen atoms of the hydrate (O_c). For comparative purposes, the O−O RDF for the pure water simulation (E) has been drawn. The first peak in the O_c−O RDF appears at ca. 2.58 Å and gives a running integration number of ca. 2. In pure water this peak is shifted by 0.22 Å and integrates to 2, as well. This shift indicates the magnitude of the increase in interaction among the water molecules of the first and second hydration shells compared to the bulk water−water interactions. There is a remarkable agreement of these figures with those obtained by Bergström et al.[50] for the hydration of Cr^{3+} in aqueous perchlorate solutions (O_I−O_{II} = 2.60 Å) using an infrared absorption double-difference method, and by Read and Sandström[46] from LAXS spectroscopy. The strong polarization of the first shell water molecules in addition to the high charge of cation are responsible for this large shrinking of the second hydration shell around the hexahydrate.

The water structure around the small and big sphere bearing triple charge is displayed in Figure 4 where the RDFs (Q3−O

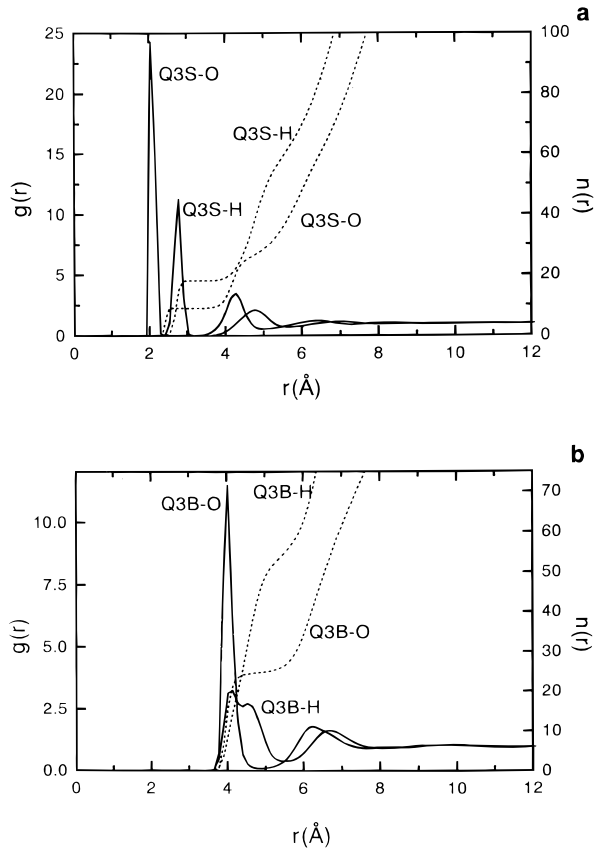

Figure 4. (a) Q3S−O and Q3S−H RDF (solid line) and their running integration numbers (dashed line) of simulation C. (b) Q3B-O and Q3B-H RDF (solid line) and their running integration numbers (dashed line) of simulation D.

and Q3−H) for simulations C and D are shown. Q3−O RDFs are illustrative of two extremes of the simple ionic solvation model. On one hand, the small sphere gives information on the first hydration shell that is represented by a sharp peak centered at 2.05 Å which integrates to nine water molecules. This overestimation of the first-shell hydration number has been previously obtained by several authors when simulating highly charged cations. This artifact has been assigned to large many-body effects.[51−53] It is worth noting that the first maximum of the Q3S−O RDF appears exactly at the same value that the minimum of the Q3S−water potential energy surface; that is, the cation−water interactions are so strong that water−water interactions do not affect the Q3S−O first shell distance. The second hydration shell for the small sphere is represented by a peak (4.26 Å) which integrates to 18 water molecules, whereas for the big sphere the RDF's maximum (4.02 Å) integrates to 25.

For the solution containing the small charged sphere, its Q3S−H RDF shows two peaks (Figure 4a); the first corresponds to 18 hydrogens and the second to ca. 44. In the case of the solution containing the big charged sphere, the Q3B−H RDF presents a wide double peak at 4−5 Å which integrates to ca. 55 hydrogen atoms (Figure 4b).

It is interesting to observe the different arrangements given by the three models of trivalent cation employed. The Q3S allows the description of the first shell, but due to the strong many-body effects the hydration number is overestimated leading to nine water molecules; obviously no information can be obtained about this region from the other two models, Q3B and HI. On the contrary, the three models supply information for the second hydration shell that is far from being similar. In fact, the model using Q3B largely overestimates the hydration number for this shell, ca. 25, with the two hydrogens of the water molecule having different, though well-defined, orientation such that a double peak at the Q3B-H RDF appears. In short, the structure is close to those of clathrates of alkali metal cations reported experimentally and theoretically.[54−56] Q3S has a second shell formed by 18 water molecules that bounds by pairs the 9 first-shell water molecules through hydrogen bonding. Thus, the specific description of the water molecules in the first shell introduces a set of preferential binding sites in the second shell region that is responsible of the structure for this shell. Nevertheless, due to the overestimation of water molecules in the first shell, the structural error is transmitted to the second shell. The change of the orientational water−cation angle, θ, with distance for these two systems also reflects the largely different arrangement of solvent molecules around the highly charged spheres. The solution containing Q3S (C in Figure 2) exhibits the largest short-range order around the cation and the smallest hump from the second shell to the bulk. The model with Q3B (D in Figure 2) shows a second shell with the smallest angle value, but where a certain preferred orientation remains for an incipient third shell, leading to a large hump at ca. 6 Å. Comparing the behavior of the orientational water angle for the different simulations, it is seen how, after ca. 8 Å, that is, beyond the ill-defined third shell, the three simulations without counterions (i.e., B, C, and D), almost overimpose. To the contrary, simulation A, which contains the hydrated ion and three chlorides, shows a strong decay of the orientational water angle at cation distances shorter than those of the other simulations. It is due to the concurrent structure-breaking effect of anions placed ca. 6 Å from the Cr^{3+}.

EXAFS Results. To investigate the possibility of the entrance of Cl^- anions in the first or second coordination sphere of Cr^{3+} cations, the X-ray absorption spectra of 0.1 *m* $Cr(NO_3)_3$ aqueous solution in 0.3 *m* HCl medium was measured. Since chlorine atoms have a small scattering power that could render this detection difficult in the second coordination sphere of Cr^{3+} ions, we investigated the hydration structure of a Cr^{3+} solution containing HBr instead of HCl in the same concentration. We replaced HCl by HBr because Br^- ions should have similar chemical behavior, but they have a higher scattering power and thus a higher backscattering amplitude in the contribution to the EXAFS spectrum. A third solution 0.3 *m* in $HClO_4$ was used as a blank since ClO_4^- anions are not reported to enter the coordination spheres of chromium at low salt concentration.[46]

The EXAFS spectra of the three solutions included in Figure 5 look quite similar. In all cases the signal-to-noise ratio is good up to $k = 15$ Å^{-1}. The imaginary and absolute parts of the Fourier transform look quite the same as well. In a previous paper we studied by EXAFS the hydration structure of Cr^{3+} solutions at pH = 1 using HNO_3 as acidifying agent in a wide range of concentrations, 0.005 − 2.6 *m*.[28b] No significant changes in the fitting parameters were detected with concentration, but in addition to the Cr−O EXAFS shell attributable to the first hydration sphere, a Cr−O contribution at $R \approx 4.0$ Å was detected, which was ascribed to a second hydration shell.[28]

The phase shift and backscattering amplitude functions used in those articles[28] to fit the EXAFS data were obtained from the experimental EXAFS function of the crystalline $[Cr(NO^3)_3]\cdot 9H_2O$, using the structural parameters obtained from an earlier X-ray determination.[57] The structural parameters of the crystalline compound have been refined on the basis of a new XRD study.[58] Taking into account the new structural parameters, the reference functions have been recalculated, which means a

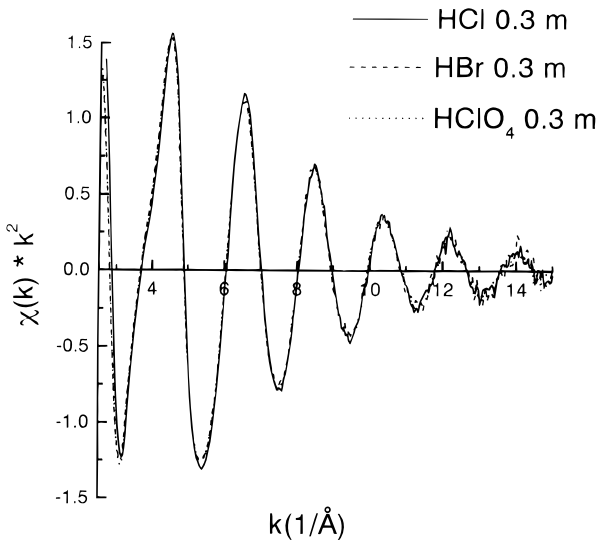

Figure 5. Raw EXAFS spectra of the Cr−K edge of the $Cr(NO_3)_3$ aqueous solutions in different media.

recalibration of the previous analysis. Moreover, using a new version (6.01) of the FEFF code, we have calculated the phase shift and backscattering amplitude functions theoretically.

The spectra of the three 0.1 *m* $Cr(NO_3))_3$ freshly prepared solutions 0.3 *m* in HCl, HBr, and HClO4, respectively, have been analyzed with the two new reference functions, one obtained from the experimental spectrum of crystalline $Cr(NO_3)_3 \cdot 9H_2O$ with a slightly shorter coordination distance (1.957 Å), and one calculated with FEFF 6.01. The values of coordination number and coordination distance obtained for the best fits have been included in Table 2. Goodness-of-fit values were between 5 and 10. (Debye−Waller factors and inner potential correction are supplied as Supporting Information. A figure including the EXAFS raw data and the best fit of the hydrochloric acid solution using the new experimental reference[58] as well as the magnitude and imaginary part of the uncorrected Fourier transform spectra is given as Supporting Information as well.)

As can be seen in Table 2, no significant changes can be detected between the parameters of the three solutions, nor in the first coordination sphere, nor in the second. Contrary to earlier attempts with a previous version of FEFF, good fits were found using the reference functions calculated with FEFF 6.01. The fitting parameters are very similar to those found when using the functions obtained from the experimental spectrum, the only difference being the higher Debye−Waller factors obtained when using the theoretical functions, which are higher than those of the experimental ones.

From all the information included in Table 2, one can conclude that the first and second coordination spheres of Cr^{3+} cations are not altered by the presence of Cl^- or Br^- anions in the solution; that is, the coherent contributions to the EXAFS function are exactly the same in the three solutions regardless of the acid that was added to them. It also must be stated that the spectrum recorded after leaving the solution equilibrating for 12 h is exactly the same as the one recorded from the freshly prepared solutions.

Translational Dynamics. *Self-Diffusion Coefficients.* A primary property to describe the mobility of a particle, *i*, in solution is the translational self-diffusion coefficient, D_i, which can be calculated from the mean-square displacement (MSD) by means of the expression:

$$D_i = \lim_{t\to\infty} \frac{\langle [\vec{r}_i(t) - \vec{r}_i(0)]^2 \rangle}{6t} \qquad (3)$$

Table 3 collects the D_i values obtained for the ions present in the solutions, as well as those corresponding to water molecules (total) and those of the second shell (2nd shell). In the first two cases, MSDs have been obtained using multiple time origins up to half of the simulation period (100 ps) in order to obtain all MSD points with equal statistics. In addition, the four statistically independent runs were averaged. Water molecules belonging to the second hydration shell were those which remained at least 20 ps inside the region defined by the minimum of the Cr−O RDF. As discussed below, this value is consistent with the mean residence time of water molecules in this shell and guarantees a displacement big enough to reach the asymptotic limit of the MSD function. The MSD of the Cr^{3+} hexahydrate corresponding to simulations A and B are displayed as Supporting Information..

The comparison of D_i values (Table 3) deserves some general comments. First of all, the mobility of the hexahydrate is reduced by the anion presence (cf. values from simulations A (with chlorides) and B (without chlorides)). Simulation B would represent the extreme case of infinite dilute solution, where the cation mobility would not be affected by an ionic atmosphere. Likewise, the change from simulation A to B may be envisaged as a formal decreasing of salt concentration, which is well known to increase the diffusion coefficient.[8,59,60] A recent MD simulation of aqueous NaCl solution has shown this concentration effect on ionic D_i values.[61]

When the chloride diffusion coefficients were calculated, a splitting in the behavior of the three anions was systematically found; two of them gave values quite similar and greater than the third one. Although, the D_i value for a system containing only chloride anions has not been obtained in this work, Perera et al.[44] obtained a value of 1.57×10^{-5} cm^2 s^{-1} for a simulation with conditions similar to ours. As found for the cation, the effect of counterions is to decrease the diffusion coefficient of the anion. Finally, the comparison between water diffusion coefficients obtained from the average of all molecules forming the solvent (H_2O_{total}) and from the molecules belonging to the second shell shows clearly how the mobility of these latter water molecules is strongly restricted by the Cr^{3+} hexahydrate.

For the particular case of aqueous $CrCl_3$ solutions, Eastel et al.,[59] using the diaphragm cell method, measured the diffusion coefficient of the components of this solution in a large range of concentrations, showing how the Cr^{3+} diffusion coefficient decreases by a factor of 5 when one goes from infinite dilute solution to 2.5 mol dm^{-3} (0.53×10^{-5} cm^2 s^{-1} for infinite dilute solution and 0.11×10^{-5} cm^2/s for $c = 2.5$ M). The value calculated by us for the hexahydrate in solution A is 0.45×10^{-5} cm^2 s^{-1}, corresponding to a concentration ca. 0.25 M. The experimental interpolated D_i value for this concentration is about 0.47×10^{-5} cm^2/s. Although the coincidence of these values could be affected by a certain degree of error cancellation, the approach of hydrated ion−water interaction potential reveals as an excellent strategy to mimic the dynamical hydration of highly charged cations. Bleuzen et al.[26] also obtain a reasonable value for the diffusion coefficient of a Cr^{3+} hexahydrate (0.53×10^{-5} cm^2/s), which seems to reinforce the validity of our hydrated ion model, although in this case the inclusion of some empirical criteria in the determination of the best fitting makes the conclusion less direct.

TABLE 2: EXAFS Coordination Parameters of 0.1 *m* $Cr(NO_3)_3$ Aqueous Solutions, 0.3 *m* in the Indicated Acids[a]

	references used						
	theoret FEFF 6.01[a,b]				exptl $Cr(NO_3)_3$ $R_{Cr-O} = 1.957$Å[c]		
		acid added			acid added		
geometrical parameters	shell	HCl	HBr	$HClO_4$	HCl	HBr	$HClO_4$
R (Cr−O)	1st	1.97	1.97	1.97	1.96	1.96	1.96
	2nd	3.91	3.91	3.90	3.87	3.91	3.91
N	1st	5.9	5.9	5.9	6.2	6.2	6.2
	2nd	13.7	13.5	14.0	14.0	13.4	14.2

[a] Fitting ranges were $\Delta k = 3-12.5$ Å^{-1} and $\Delta R = 0$-5 Å. Standard deviations were 0.1 ($Cr-O_I$) and 0.7 ($Cr-O_{II}$), and 0.008 Å ($Cr-O_I$) and 0.04 Å ($Cr-O_{II}$), for coordination numbers and distances, respectively. [b] Taken from ref 32. [c] Taken from ref 58.

TABLE 3: Translational Self-Diffusion Coefficients, D_i (in 10^{-5} cm^2 s^{-1})[a]

	simulation		
species	A	B	E
$[Cr(H_2O)_6]^{3+}$	0.45	0.68	
Cl^-	1.27, 0.79[b]		
$H_2O_{2nd\ shell}$	0.77	0.93	
H_2O_{total}	3.05	3.26	3.40

[a] Average estimated errors are *ca.* 23% ($[Cr(H_2O)_6]^{3+}$ and Cl^-), 10% ($H_2O_{2nd\ shell}$), and 7% (H_2O_{total}). [b] The first value corresponds to two chlorides and the second value to the third one.

For the chloride anion, the interpolated experimental diffusion coefficient obtained by Eastel et al.[59] is 1.59×10^{-5} cm^2 s^{-1}, whereas our theoretical value is 1.1×10^{-5} cm^2 s^{-1}. The recent MD study of Lyubartsev and Laaksonen[61] for NaCl with a similar simulation time, treatment for the long-range electrostatic forces, and number of water molecules gives a D_{Cl^-} value of 1.2×10^{-5} cm^2 s^{-1}. Concerning water molecules mobility, the TIP4P model overestimates the diffusion coefficient.[62,63] Simulation A gives a mean value of 3.1×10^{-5} cm^2 s^{-1} versus the experimental one of 2.0×10^{-5} cm^2 s^{-1}.[59] Anyway, it is useful to compare the order of magnitude of the difference between the difffusion coefficients of a water molecule in the bulk and in the second hydration shell. Eastel et al.[59] assumed that the D_{H_2O-2nd} value may be the algebraic mean of the values corresponding to the D values for water molecules in the bulk and in the first shell, this latter for Cr^{3+} hydration being equal to $D_{Cr^{3+}}$. If this criteria had been used with data of Table 3, the estimated D_{H_2O-2nd} would have been 1.8×10^{-5} cm^2 s^{-1} instead of that shown, 0.8×10^{-5} cm^2 s^{-1}. This value indicates that mobility of second hydration shell water molecules behaves following a ratio 85:15 (first-shell:bulk). In other words, for this trivalent metallic cation the second hydration shell is tighter joined to the first hydration shell than to the bulk water molecules.

To check the validity of the diffusion coefficients obtained for the different particles, they were also estimated from the integration of their corresponding velocity autocorrelation function (VAC).[1,44] Results are similar to those obtained from the MSD method and confirm the precedent analysis.

It is interesting to examine the Fourier transform $f_v(\omega)$ of the VAC, called either power spectrum or spectral density that in this case may be associated with the hindered translational motion of the corresponding particle. The spectra measured by various spectroscopic techniques are the power spectra of well-defined dynamical variables.[64] Figure 6 compares the spectral densities of the hindered translations of water molecule in pure water (simulation E) and in the second hydration shell of Cr^{3+} (simulation A). The curve for pure water shows a first peak at ca. 50 cm^{-1} that has been assigned to hydrogen bond bending (O−O−O flexing) motions and a second broad peak

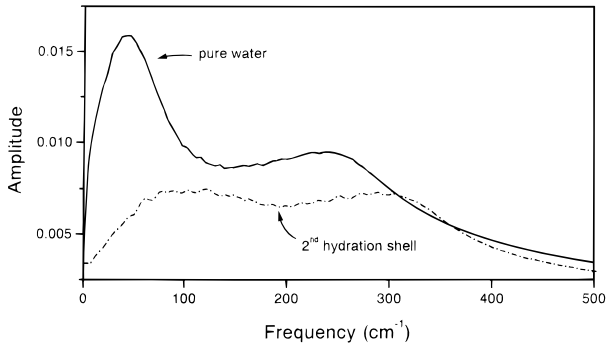

Figure 6. Fourier transform of velocity autocorrelation function. Power spectrum for pure water simulation (solid line) and water molecules of the second hydration shell of the Cr^{3+} hexahydrate, simulation A (dashed line).

at ca. 250 cm^{-1} assignable to O−O stretching motions.[65] Bertolini et al. have previously shown quite a similar spectra from MD simulations using 343 TIP4P water molecules.[66] Given the low concentration, the spectral densities for all water molecules in the salt solution is quite similar to that of pure water. More interestingly, the power spectrum corresponding to the second hydration shell of Cr^{3+} shows a shift toward higher frequencies of the two peaks; the hydrogen bond bending appears about 100 cm^{-1} and the O−O stretching motions about 300 cm^{-1}. Both displacements reflects how this second hydration shell is strongly attached to the hydrated ion. The changes observed in the spectrum can be considered of the same order than those obtained for the first hydration shell of small monovalent cations as Li^+ and Na^+.[67,68]

Interdiffusion Coefficients. In addition to the individual mobility of the particles, the relative motion of ions is important in the definition of physicochemical properties of electrolyte solution, such as association rate of ions or equivalent conductivity.[5,61] The interdiffusion coefficient is defined by the following expression:

$$D_{12} = kT\frac{m_1 + m_2}{2m_1m_2}\int_0^\infty J(t)\,\mathrm{d}t \qquad (4)$$

where $J(t)$ represents a normalized current correlation function defined as

$$J(t) = \frac{\langle \vec{j}(t)\vec{j}(0)\rangle}{\langle |\vec{j}(0)|^2\rangle} \qquad (5)$$

The vector $\vec{j}(t) = \sum_i q_i\vec{v}_i(t)$ is the summation of the contributions to the current flow due to all ions present in the system.[61,69] In a general way, the interdiffusion coefficient is a measure of the degree of mutual dependence of the ions; thus if they move independently from their counterions, D_{12} takes the value of the arithmetic mean of their corresponding self-diffusion coef-

TABLE 4: Rotational Correlation Times for $l = 1$and $l = 2$, and Rotational Diffusion Coefficients of $[Cr(H_2O)_6]^{3+}$ for Simulations of the Hexahydrate with (A) and without (B) Chlorides[a]

			D_R (ps^{-1}) calculated from C_l	
simulation	τ_1 (ps)	τ_2 (ps)	$C_1(t)$	$C_2(t)$
A	180.2	60.2	0.0028	0.0028
B	153.1	51.2	0.0033	0.0033

[a] Average estimated errors are *ca.* 25%.

ficients. Otherwise, the value indicates the degree of correlation among the ions and may represent an estimation of certain ion−ion associations.[70] From simulation A, D_{12} has been calculated considering the hexahydrate cation and the three halide anions, its value being $0.49 \pm 0.13 \times 10^{-5}$ cm^2 s^{-1}. The comparison of this result with the value of D for the Cr^{3+} hexahydrate and chlorides in Table 3 indicates a large mutual dependence among the ions. Using similar simulation conditions to those here employed, Lyubartsev and Laaksonen obtain for an aqueous NaCl solution a much smaller ionic interdependency.[61]

Orientational Dynamics. To complete the description of the dynamical properties, reorientational motions of the hexahydrate and water molecules have also been considered. This type of information may be obtained by a set of reorientational time correlation functions defined as

$$C_l^i(t) = \langle P_l(\vec{u}_i(0)\vec{u}_i(t))\rangle \tag{6}$$

where P_l is the lth Legendre polynomial and $\vec{u}_i$ is a unit vector that characterizes the orientation of the molecule. $C_l(t)$ values are computed with respect to a coordinate frame fixed on the molecule. These correlation functions are related to spectroscopic measurements: IR line shapes are determined by $l = 1$ correlation functions and Raman line shapes and NMR relaxation times by $l = 2$ functions.[1,7]

Alternatively, orientational dynamics may be examined from the angular velocity autocorrelation function (AVAF), defined as

$$C_{\omega i}(t) = \frac{\langle \omega_i(0)\, \omega_i(t)\, \vec{u}_i(0)\, \vec{u}_i(t)\rangle}{\langle \omega_i^2\rangle} \tag{7}$$

where ω_i and $\vec{u}_i$ represents the magnitude and unit vector of the angular velocity, respectively, and the averages are over a set of given molecules and over a suitable range of initial times.

To examine the rotational properties of the hexahydrate, the fixed molecular frame chosen for the $[Cr(H_2O)_6]^{3+}$ has been based on three Cr−O vectors that are perpendicular among themselves. The high symmetry of the cluster (spherical top) makes the three components completely equivalent, so averages of them are always considered in the analysis. Table 4 collects the results obtained for the hexahydrate, showing longer reorientation times for the cluster under the influence of the chloride anions. (Plots of the reorientational correlation functions for the hexahydrate are given in the Supporting Information.) Two basic reasons with opposite effects could be invoked to explain the ionic atmosphere effect on the rotation of the hydrated ion. The first one is the disruption produced by anions on the water structure adapted to the interaction with the cation, which could lead to an enhancement for rotation of the hydrate. The second basic reason is the local electric field created by ions. Under its influence the multipole charge distribution of hexahydrate retains certain preferential orientations that delay the rotation.

TABLE 5: Reorientation Times (ps) of Water Molecules in the Second Hydration Shell of Cr^{3+} for Simulations with (A) and without (B) Chlorides, and in Pure Water (Simulation E)[a]

type of water/ simulation	τ_{1x}	τ_{1y}	τ_{1z}	τ_{2x}	τ_{2y}	τ_{2z}
2nd shell/A	5.2		4.1	3.1		2.1
2nd shell/B	3.8		3.4	3.0		1.8
bulk/E	3.7	3.6	2.6	2.0	1.7	1.6

[a] Average estimated errors are *ca.* 12% (2nd shell) and 2%(bulk). (Axis are indicated in Scheme 1).

SCHEME 1

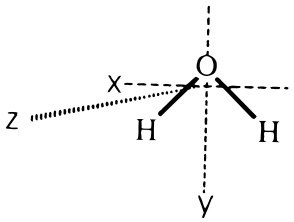

An important conclusion derived from the values of rotational correlation times for the hexahydrate is that the Debye rotation diffusion model is perfectly followed, i.e., $\tau_1/\tau_2 = 3$.[64] On the basis of this model, these data yield the rotational diffusion coefficient D_R, which is independent of l, calculated by the following equation

$$\tau_l^{-1} = -\frac{\partial}{\partial t} \ln C_l(t) \equiv l(l+1)D_R \tag{8}$$

D_R values are given in Table 4. τ_2 can be compared with the experimental reorientational times obtained by ^1H NMR. The values found in the literature cover the range 40−85 ps.[71] The agreement is particularly satisfactory taking into account that the imposed rigidity of our model can be one of the main drawbacks that could be argued. The similarity between the experimental and theoretical τ_2 values indicates that the Cr^{3+} hexahydrate, that is, the central cation and the six oxygens of its first hydration shell, rotate almost like a rigid solid, and that the HIW potential supplies satisfactory mean interaction forces with the surrounding water shells.

Rotational diffusion coefficients can also be computed using the AVAF. The obtained values are 0.0029 and 0.0032 ps^{-1} for simulations A and B, respectively. When these results are compared with those computed by means of $C_l(t)$'s functions, discrepancies are below 4%.

Concerning orientational dynamics of water molecules, Scheme 1 depicts the three main axes describing the rotational motion of water molecules. As in the case of translational diffusion motion, analysis is centered on the observed differences between second hydration shell water molecules and those belonging to the pure water simulation. The different $C_2(t)$ functions are shown in the Supporting Information. Reorientation times are collected in Table 5. Clear tendencies can be observed in this table. First of all, water molecules belonging to the second hydration shell take more time in the reorientation process than those of the pure water simulation, reflecting again the strong influence of the hexahydrate. This effect is especially dramatic in the case of the vector y (dipole moment of water molecule) for which it is not possible to fit a single exponential decay, due to the strong hindrance for rotation of this axis. Simulations with and without chloride anions show differences as well. In this sense, the presence of chloride ions increases the reorientation times of water molecules. This effect is parallel

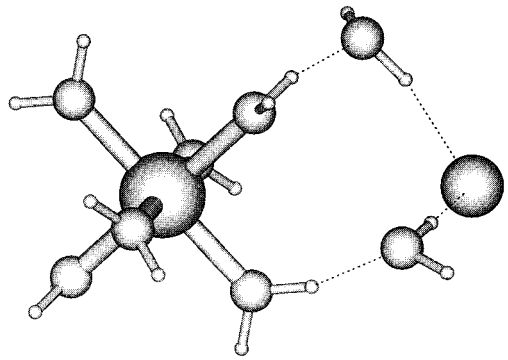

Figure 7. Random snapshot taken from simulation A showing the existence of bridging water molecules between the hexahydrate and chloride ions.

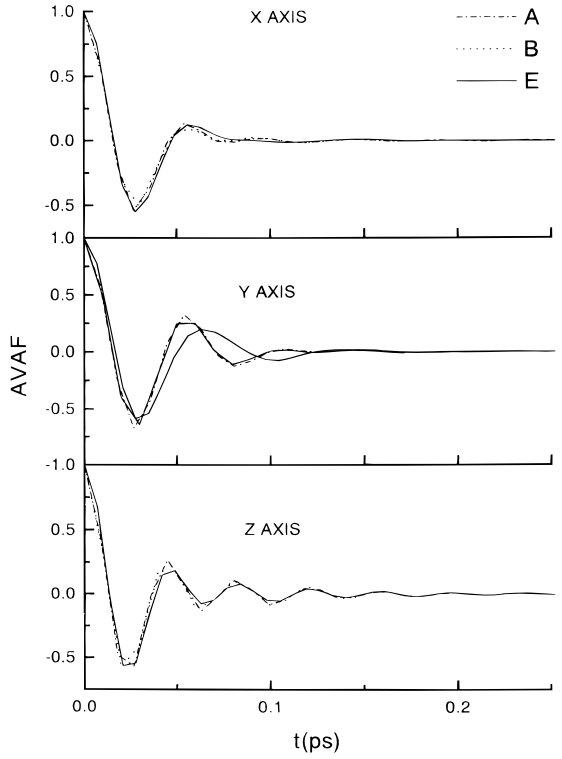

Figure 8. Components of the angular velocity autocorrelation function (AVAF) for water molecules of the second hydration shell of Cr^{3+} in simulations A and B, and that of free water molecules in simulation E.

to that observed in the case of the Cr^{3+} hexahydrate and may be explained, at least partially, by the existence of favorable arrangements in which the hexahydrate and the Cl^- are bridged through water molecules, which interact favorably with both ions. This can be visualized in Figure 7 where a random configuration is shown.[72] This advantageous situation has been detected for the three Cl^- ions by means of a systematic investigation of the chlorine nearest neighborhood; 90% of the examined configurations showed these bridged structures, which were characterized by Cr−Cl distances shorter than 6.3 Å. Possibly, these bridging water molecules contribute to the slower reorientation of the hexahydrate in the presence of the anions as well. In all cases, Table 5 shows strong deviations from the predictions of the Debye model as the τ_1/τ_2 ratio is quite different from 3.

An alternative view of the strong hindrance for rotation of dipole water axis in the second hydration shell may be obtained by examining AVAFs. Figure 8 shows the molecule fixed frame components (see Scheme 1) of the angular velocity autocorrelation function. The *y* component shows the main differences, autocorrelation functions of simulations A and B are more structured than that of pure water (simulation E). This reveals that there is a librational movement component for the water molecules in the second hydration shell larger than for bulk water molecules.

TABLE 6: Mean Residence Time (ps) of Water Molecules in the Second Hydration Shell of the Cr^{3+} Hexahydrate and in the First Hydration Shell of Cl^-[a]

ion	simulation	τ ($t^* = 0$ ps)	τ ($t^* = 2$ ps)
$[Cr(H_2O)_6]^{3+}$	A (with Cl^-)	7	31
$[Cr(H_2O)_6]^{3+}$	B (without Cl^-)	6	32
Cl^-	A	4	11

[a] (For definition of t^*, see text). Average estimated errors are *ca.* 20%.

Residence Time. The concept of hydration number, as it raises from the radial distribution function, is defined exclusively on the basis of static quantities in the equilibrium. However, a deeper insight into the concept can be obtained from dynamical information, recognizing the microscopical structure of the solvation phenomenon and finding out how much time a water molecule is retained in a given hydration shell around a solute. The mean residence time is based on the definition of a function $n_{ion}(t)$ which measures the number of molecules which are in a given region around the ion after a period of time *t*. From this definition, $n_{ion}(0)$ is the number of water molecules in a given region; that is, if this region is the first hydration shell; $n_{ion}(0)$ represents the dynamic hydration number of the first shell. Excluding an initial period for which the function decays rapidly, $n_{ion}(t)$ adopts an exponential form, i.e., $n_{ion}(t) \sim e^{-t/\tau}$, where τ represents a correlation or relaxation time characteristic of the persistence of water molecules in a given region around the ion. This quantity τ is defined as the residence time of water molecules in that region. Calculations of τ have been carried out using the method proposed by Impey et al.,[73] where

$$n_{ion}(t) = \frac{1}{N_t}\sum_{n=1}^{N_t}\sum_{j} P_j(t_n,t;t^*) \qquad (9)$$

and $P_j(t_n,t;t^*)$ is a function that can take only a value of 1 if water molecule *j* lies within the region considered at both time steps t_n and $t + t_n$ not leaving in the meantime the region for a period longer than t^*; otherwise, P_j takes a value of 0. In this work, mean residence times have been computed using two different values of t^* since there is a certain degree of uncertainty to deal with a physically well-founded value for t^*. The first was 2 ps, as used by Impey et al. method,[73] and the second was 0 ps, as adopted by Garcia and Stiller.[74] From the definition of t^* it is clear that the second value will lead to smaller residence times than the first one, and therefore the results here presented may be considered as the limiting values of a range that should contain reasonably the experimental residence times. Table 6 collects the values obtained for the second hydration shell of the hydrated cation and the first shell of the anion. The residence time of a water molecule in the hydration shell of the Cr^{3+} hexahydrate is in the range 10−30 ps, which represents a typical value of this magnitude for the first shell of many monovalent and some divalent cations; i.e., this second hydration shell is as defined as many other first hydration shells.[7] Thus, this quantity supports a posteriori the use of the hydrated ion model to describe the Cr^{3+} hydration. Bleuzen et al.,[26] on the hydration of this cation, find from NMR data a value of 128 ps which compares well with an estimated

value from MD simulations of 144 ps. Due to the discrepancy in this value, we have carefully examined the evaluation of this magnitude, and the effect on its calculation caused by the consideration of different radii to define the second shell region. Those authors[26] find that their method of calculation of residence time is quite dependent on the radius definition, so that changes of 0.1 Å lead to changes in the residence time value of one order of magnitude.[75] The methods of calculation employed in the present work are relatively independent on the radius definition for small changes. Thus, lengthenings of 0.1−0.2 Å involve changes in the values of the mean residence time in the order of 1 ps. Significant dependency appears when reducing the radius by 0.3−0.4 Å, but, as can be seen in RDF of Figure 1, it clearly implies a bad choice of the second hydration shell region. Comparison of residence times for water molecules around the hexahydrate for simulations with and without counterions indicates that this magnitude is not affected by the presence of Cl^-.

Concerning water molecules solvating chloride anions, their residence time is found to take similar values to those determined theoretical and experimentally for different electrolytes (3−10 ps).[7,61,74] According to their average location with respect to the cation, it seems that the dynamics of water release from its hydration shell is not too much affected by it. Although this fact could seem to be contrary to the existence of bridging water molecules, the wide range of mean residence time and the loss of water structure in that region make both explanations compatible.

Concluding Remarks

The use of the hydrated ion represents a chemical approach to the study of ion solvation of monatomic cations of particular complexity. It may be regarded as an implementation of the old electrochemistry concept of the hydrated ion (solventberg unit) in statistical simulations.

The structural and dynamical properties obtained for the Cr^{3+} aqueous solutions using molecular dynamics, joined to the energetics and structural properties previously reported by Monte Carlo simulations,[23] lead us to conclude that the hydrated ion−water interaction potential represents a fruitful approach to describe ionic solutions of particularly conflicting highly charged cations. It is worth pointing that this first-principle interaction potential is able to predict, quite reasonably and simultaneously, properties as different as hydration energy, ion−water RDF, translational self-diffusion coefficient, rotational correlation time, and mean residence time of water molecules, without the inclusion of any change either in the functional form or in the values of parameters defining the potential. At the current state of development, the two main drawbacks are (a) the computational effort and the intrinsic difficulty to develop such interaction potentials, which makes the dissemination of these types of potentials not easy, and (b) the rigidity of the first hydration shell. Although this precludes a detailed information of the first-shell dynamics, many properties of ionic aqueous solutions are independent on these shortcomings and the important ionic atmosphere effects on physicochemical properties of chemical systems in solution as well.

Bearing in mind the results obtained for the small and big charged soft spheres, the hydrated ion represents a compromise among these two simpler models of cation. The apriority of the hexahydration for the trivalent cation avoids the collapse of the first shell structure, with a hydration number of 9, observed for the small highly charged sphere. On the other hand, it guarantees a reasonable definition of specific interaction zones in the region beyond the first coordination sphere, contrary to the clathrate-like structure induced for the big sphere in its second hydration shell.

EXAFS measurements of a dilute $CrCl_3$ aqueous solution have shown that chloride anions are placed beyond the second hydration region. RDFs confirm this finding and suggest they are in an ill-defined third hydration shell. The presence of anion decreases the values of the translational and rotational diffusion coefficients of the Cr^{3+}.

Given that the Cr^{3+} hexahydrate is the most representative example of a hydrated ion, the rigid approach seems to be particularly adequate as shown; the strict verification of the Debye rotation model allows the suggestion of an alternative definition of a hydrated ion in rotational terms: An ion in water can be considered as forming a well-defined hydrated ion if its hydrate rotates following the Debye rotation model.

Acknowledgment. We thank the Centro Informático Científico de Andalucía for providing us the experimental use of its parallel CONVEX-Exemplar SPP-1000 Series to carry out the MD simulations. Photon Factory staff, Tsukuba, is acknowledged for beamtime allocation, as well as Professor Watanabe and Drs. Miyanaga and Sakane for their cooperation during measuring time. Likewise, we thank Dr. A. E. Garcia, Los Alamos National Laboratory, and Dr. A. P. Lyubartsev, Arrhenius Laboratory (Stockholm), for useful suggestions in performing the statistical analysis. J.M.M. thanks K.R. for his hospitality during his stay at Oxford University. This work was partially supported by funds of the DGICYT of Spain (PB 95-0549).

Supporting Information Available: Tables of coefficients for the HIW, HICI, and soft-sphere potentials and EXAFS coordination parameters of $Cr(NO_3)_3$ aqueous solutions and figures of EXAFS raw data and best fit parameters, MSD of the hexahydrate ion with and without Cl^- anions, and first and second Legendre polynomial time correlation functions for $[Cr(H_2O)_6]^{3+}$ and water molecules (7 pages). See any current masthead page for ordering information and Web access instructions.

References and Notes

(1) Allen, M. P.; Tildesley, D. J. *Computer Simulations of Liquids*; Oxford University Press: Oxford, 1987.
(2) Hermann, D. W. *Computer Simulation Methods*, 2nd ed.; Springer-Verlag: Berlin, 1990.
(3) Clementi, E., Ed. *Modern Techniques in Computational Chemistry*; Escom: Leiden, 1991.
(4) Simkin, B. Ya; Sheikhet, I. I. *Quantum Chemical and Statistical Theory of Solutions: A Computational Approach*; Ellis Horwood: London, 1995, Chapter 4.
(5) Wolynes, P.G. *Annu. Rev. Phys. Chem.* **1980**, *31*, 345.
(6) (a) Marcus, Y. *Ion Solvation*; Wiley: Chichester, 1986. (b) Marcus, Y. *Chem. Rev.* **1988**, *88*, 1475.
(7) Ohtaki, H.; Radnai, T. *Chem. Rev.* **1993**, *93*, 1157.
(8) Bockris, J. O'M.; Reddy, A. K. N. *Modern Electrochemistry*; Plenum: New York, 1973; Vol. 1.
(9) Conway, B. E. *Ionic Hydration in Chemistry and Biophysics*; Elsevier: Amsterdam, 1981.
(10) Krestov, G. F. *Thermodynamics of Solvation*; Ellis Horwood: Chichester, 1991.
(11) Elrod, N. J.; Saykally, R. J. *Chem. Rev.* **1994**, *94*, 1975.
(12) Marini, G. W.; Texler, N. R.; Rode, B. M. *J. Phys. Chem.* **1996**, *100*, 6808 and references therein.
(13) Bernal-Uruchurtu, M. I.; Ortega-Blake, I. J. *Chem. Phys.* **1995**, *103*, 1588.
(14) Rustad, J. R.; Hay, B. P.; Halley, J. W. *J. Chem. Phys.* **1995**, *102*, 427.
(15) Kowall, Th.; Foglia, F.; Helm, L.; Merbach, A. E. *J. Am. Chem. Soc.* **1995**, *117*, 3790.
(16) (a) Floris, F.; Persico, M.; Tani, A.; Tomasi, J. *Chem. Phys. Lett.* **1992**, *199*, 518. (b) Floris, F.; Persico, M.; Tani, A.; Tomasi, J. *Chem. Phys.* **1995**, *195*, 207.

(17) Cordeiro, M. N. D. S.; Gomes, J. A. N. F. *J. Comput. Chem.* **1993**, *14*, 629.
(18) Periole, X.; Allouche, D.; Daudey, J. P.; Sanejouand, Y. H. *J. Phys. Chem.* **1997**, *101*, 5018.
(19) Burgess, J. *Metal Ions in Solution*; Ellis Horwood: Chichester, 1978, Chapter 12.
(20) Krestov, G. A.; Novosyolov, N. P.; Perelygin, I. S.; Kolker, A. M.; Safonova, L. P.; Ovchinnikova, V. D.; Trostin, V. N. *Ionic Solvation*; Ellis Horwood: Chichester, 1994, Chapter 5.
(21) Frank, H. S. ; Evans, M. W. *J. Chem. Phys.* **1945**, *13*, 507.
(22) Pappalardo, R. R.; Sánchez Marcos, E. *J. Phys. Chem.* **1993**, *97*, 4500.
(23) Pappalardo, R. R.; Martínez, J. M.; Sánchez Marcos, E. *J. Phys. Chem.* **1996**, *100*, 11748.
(24) Sánchez Marcos, E.; Martínez, J. M.; Pappalardo, R. R. *J. Chem. Phys.* **1996**, *105*, 5968.
(25) Roux, B.; Yu, H.; Karplus, M. *J. Phys. Chem.* **1990**, *94*, 4683.
(26) Bleuzen, A.; Foglia, F.; Furet, E.; Helm, L.; Merbach, A. E.; Weber, J. *J. Am. Chem. Soc.* **1996**, *118*, 12777.
(27) Wasserman, E.; Rustad, J. R.; Xantheas, S.S. *J. Chem. Phys.* **1997**, *106*, 9769.
(28) (a) Muñoz-Páez, A.; Sánchez Marcos, E. *J. Am. Chem. Soc.* **1992**, *114*, 6931. (b)Muñoz-Páez, A.; Pappalardo, R. R.; Sánchez Marcos, E. *J. Am. Chem. Soc.* **1995**, *117*, 11710.
(29) Díaz-Moreno, S.; Muñoz-Páez, A.; Martínez, J. M.; Pappalardo, R. R.; Sánchez Marcos, E. *J. Am. Chem. Soc.* **1996**, *118*, 12654.
(30) (a) Sánchez Marcos, E.; Gil, M.; Martínez, J. M.; Muñoz-Páez, A.; Sánchez Marcos, A. *Rev. Sci. Instrum.* **1994**, *65*, 2153. (b) Muñoz-Páez, A.; Gil, M.; Martínez, J. M.; Sánchez Marcos, E. *Physica B* **1995**, *208, 209*, 241.
(31) Vaarkamp, M.; Linders, J.C.; Koningsberger, D.C. *Physica B* **1995**, *208, 209*, 159.
(32) Rehr, J. J.; Mustre de León J.; Zabinsky, S. I.; Albers, R. C. *J. Am. Chem. Soc.* **1991**, *113*, 5135.
(33) Lytle, F. W.; Sayers, D. E.; Stern, E. A. *Physica B* **1988**, *158*, 701.
(34) Jorgensen, W. L.; Impey, R. W.; Chandrasekhar, J.; Madura, J. D.; Klein, M. L. *J. Chem. Phys.* **1983**, *79*, 926.
(35) Matsuoka, O.; Clementi, E.; Yoshimine, M. *J. Chem. Phys.* **1976**, *64*, 1351.
(36) Chandrasekhar, J.; Spellmeyer, D. C.; Jorgensen, W. L. *J. Am. Chem. Soc.* **1984**, *106*, 903.
(37) Water basis sets were the same as in ref 23.
(38) Refson, K. *Moldy User's Manual Rev. 2.10.* Moldy code can be obtained from the CCP5 program library.
(39) Beeman, D. *J. Comput. Phys.* **1976**, *20*, 130.
(40) Refson, K. *Physica B* **1985**, *131*, 256.
(41) Goldstein, H. *Classical Mechanics* 2nd ed.; Addison-Wesley: Reading, MA, 1980.
(42) Madura, J. D.; Pettitt, B. M. *Chem. Phys. Lett.* **1988**, *150*, 105.
(43) Roberts, J. E.; Schnitker, J. *J. Phys. Chem.* **1995**, *99*, 1322.
(44) Perera, L.; Essmann, U.; Berkowitz, M. L. *J. Chem. Phys.* **1995**, *102*, 450.
(45) Quentrec, B.; Brot, C. *J. Comput. Phys.* **1975**, *13*, 430.
(46) Read, M. C.; Sandström, M. *Acta Chem. Scand.* **1992**, *46*, 1177.
(47) Caminiti, R.; Licheri, G.; Piccaluga, G.; Pinna, G. *J. Chem. Phys.* **1978**, *69*, 1.
(48) Broadbent, R. D.; Neilson, G. W.; Sandström, M. *J. Phys.: Condens. Matter* **1992**, *4*, 639.
(49) Meier, W.; Bopp, Ph.; Probst, M.M.; Spohr, E.; Lin, J.-I. *J. Phys. Chem.* **1990**, *94*, 4672.
(50) Bergström, P-A.; Lindgren, J.; Read, M.; Sandström, *J. Phys. Chem.* **1991**, *95*, 7650.
(51) (a) Probst, M. M.; Spohr, E.; Heinzinger, K. *Chem. Phys. Lett.* **1989**, *161*, 405. (b) Probst, M. M.; Spohr, E.; Heinzinger, K. *Mol. Simul.* **1991**, *7*, 43.
(52) González-Lafont, A.; Lluch, J. M.; Oliva, A.; Bertrán, J. *Chem. Phys.* **1987**, *111*, 241.
(53) Curtiss, L. A.; Halley, J. W.; Hautman, J.; Rahman, A. *J. Chem. Phys.* **1987**, *86*, 2319.
(54) Selinger, A.; Castleman, A. W., Jr. *J. Chem. Phys.* **1991**, *95*, 8442.
(55) Cioslowski, J.; Nanayakkara, A. *Int. J. Mod. Phys. B* **1992**, *23, 24*, 3687.
(56) Lipkowski, J. *Annu. Rep. Prog. Chem. Phys. Chem.* **1996**, *92C*, 307.
(57) Kannan, K. K.; Viswamitra, M. A. *Acta Crystallogr.* **1965**, *19*, 151.
(58) Lazar, D.; Ribar, B.; Divjakovic, V.; Meszaros, C. S. *Acta Crystallogr.* **1991**, *47*, 1060.
(59) Eastel, A. J.; Mills, R.; Woolf, L. A. *J. Phys. Chem.* **1989**, *93*, 4968.
(60) Miller, D. G.; Rard, J. A.; Eppstein, L. B.; Albright, J. G. *J. Phys. Chem.* **1984**, *88*, 5739.
(61) Lyubartsev, A. P.; Laaksonen, A. *J. Phys. Chem.* **1996**, *100*, 16410.
(62) Ferrario, M.; Tani, A. *Chem. Phys. Lett.* **1985**, *121*, 182.
(63) Neuwman, M. *J. Chem. Phys.* **1986**, *85*, 1567.
(64) Hansen, J. P.; McDonald, I. R. *Theory of Simple Liquids* 2nd ed.; Academic Press: London, 1990.
(65) (a) Sceats, M. G.; Rice, S. A. *J. Chem. Phys.* **1980**, *72*, 3236. (b) Bopp. P. *Pure Appl. Chem.* **1987**, *59*, 1071.
(66) Bertolini, D.; Grigolini, P.; Tani, A. *J. Chem. Phys.* **1989**, *91*, 1191.
(67) Szász, G. Y.; Heinzinger, K. *J. Chem. Phys.* **1983**, *79*, 3467.
(68) Guàrdia E.; Padró, J. A. *J. Phys. Chem.* **1990**, *94*, 6049.
(69) Hansen, J. P.; Joly, F.; McDonald, I. R. *Physica. A* **1985**, *132*, 472.
(70) Payne, V. A.; Forsyth, M.; Ratner, M. A.; Shriver, D. F.; de Leeuw, S. W. *J. Chem. Phys.* **1994**, *100*, 5201.
(71) Bloembergen, N.; Morgan, L. O. *J. Chem. Phys.* **1961**, *34*, 842. Hausser, R.; Noack, F. *Z. Phys.* **1964**, *182*, 93.
(72) Schaftenaar, G. *MOLDEN: A Portable Electron Density Program*, QCPE Program 619; *QCPE Bull.* **1992**, *12*, 3.
(73) Impey, R. W.; Madden, P. A.; McDonald, I. R. *J. Phys. Chem.* **1983**, *87*, 5071.
(74) García, A. E.; Stiller, L. *J. Comput, Chem.* **1993**, *14*, 1396.
(75) In ref 26 there seems to be a typographical error in the explanation of the changes in the mean residence time when changing the radius. The expected behavior is opposite to that indicated in the reference.